Cancer Cell
Article

The Wip1 Phosphatase Acts as a Gatekeeper in the p53-Mdm2 Autoregulatory Loop

Xiongbin Lu,[1,4,*] Ou Ma,[1] Thuy-Ai Nguyen,[1,2] Stephen N. Jones,[5] Moshe Oren,[6] and Lawrence A. Donehower[1,2,3,*]
[1]Department of Molecular Virology and Microbiology
[2]Interdepartmental Program in Cell and Molecular Biology
[3]Department of Molecular and Cellular Biology
Baylor College of Medicine, Houston, TX 77030, USA
[4]Department of Biological Sciences, University of South Carolina, Columbia, SC 29208, USA
[5]Department of Cell Biology, University of Massachusetts Medical School, Worcester, MA 01655, USA
[6]Department of Molecular Cell Biology, The Weizmann Institute, Rehovot 76100, Israel
*Correspondence: xlu@biol.sc.edu (X.L.), larryd@bcm.tmc.edu (L.A.D.)
DOI 10.1016/j.ccr.2007.08.033

SUMMARY

The tumor suppressor p53 is a transcription factor that responds to cellular stresses by initiating cell cycle arrest or apoptosis. One transcriptional target of p53 is Mdm2, an E3 ubiquitin ligase that interacts with p53 to promote its proteasomal degradation in a negative feedback regulatory loop. Here we show that the wild-type p53-induced phosphatase 1 (Wip1), or PPM1D, downregulates p53 protein levels by stabilizing Mdm2 and facilitating its access to p53. Wip1 interacts with and dephosphorylates Mdm2 at serine 395, a site phosphorylated by the ATM kinase. Dephosphorylated Mdm2 has increased stability and affinity for p53, facilitating p53 ubiquitination and degradation. Thus, Wip1 acts as a gatekeeper in the Mdm2-p53 regulatory loop by stabilizing Mdm2 and promoting Mdm2-mediated proteolysis of p53.

INTRODUCTION

The tumor suppressor p53 is a transcription factor that responds to an array of cellular stresses by initiating cell cycle arrest, DNA repair, or apoptosis (Harris and Levine, 2005). These antiproliferative p53 activities prevent a damaged cell from dividing before completion of repair and potentially becoming cancerous (Lane, 2005). The importance of p53 in maintaining genomic stability is illustrated by the fact that more than half of all human cancers lose p53 function through mutation or deletion of the *p53* gene (Martin et al., 2002). After DNA damage, p53 undergoes multiple posttranslational modifications that increase p53 stability and activate it as a potent transcription factor (Appella and Anderson, 2001; Bode and Dong, 2004; Lavin and Gueven, 2006). Activated p53 alters gene transcription patterns that result in engagement of DNA damage response and antiproliferative pathways that promote DNA repair and prevent cell cycle progression (Harris and Levine, 2005; Vogelstein et al., 2000).

One transcriptional target of p53 is the *Mdm2* gene, which encodes an E3 ubiquitin ligase (Bond et al., 2005; Michael and Oren, 2003). Mdm2 interacts with p53 and mediates its ubiquitination, resulting in p53 proteasomal degradation (Michael and Oren, 2003). Thus, Mdm2 is activated by p53 and in turn destabilizes it as part of an oscillating negative feedback regulatory loop (Bond et al., 2005). Given the ability of Mdm2 to suppress p53, it is not surprising that it is an important oncogene in its own right. A significant number of human cancers exhibit *Mdm2* gene amplification and/or overexpression (Momand et al., 1998). The *p53* gene is rarely mutated in these cancers, suggesting that Mdm2 is primarily oncogenic as a result of its ability to suppress p53 activity (Momand et al., 1998).

SIGNIFICANCE

The p53 tumor suppressor is mutated or lost in roughly half of all human cancers. In some human cancers where p53 remains structurally intact, p53 loss of function can be mediated by amplification and overexpression of the *Mdm2* gene. Mdm2 is a p53-transactivated E3 ubiquitin ligase that promotes p53 degradation in a negative feedback regulatory loop. Here we show that Wip1 acts as a molecular gatekeeper in the Mdm2-p53 autoregulatory loop by downregulating p53 via stabilization of Mdm2. This inhibition of p53 by Wip1 is consistent with observations that the *Wip1* gene is amplified and overexpressed in several human tumor types and is oncogenic in rodent fibroblast transformation assays, providing a molecular mechanism for Wip1 oncogenicity.

One aspect of the p53-Mdm2 autoregulatory loop is that, immediately following DNA damage, both p53 and Mdm2 are phosphorylated by ATM (ataxia telangiectasia mutated) and other kinases in a manner that prevents Mdm2 from interacting with p53, ensuring p53 stabilization (Canman et al., 1998; Maya et al., 2001; Tibbetts et al., 1999). DNA damage-activated ATM and ATR (ataxia telangiectasia and Rad-3-related) directly phosphorylate p53 at serine 15 and indirectly at serine 20 via activation of the Chk1 and Chk2 kinases (Canman et al., 1998; Chehab et al., 2000; Hirao et al., 2000; Tibbetts et al., 1999). ATM also phosphorylates serine 395 on Mdm2 (Maya et al., 2001). These phosphorylations of p53 and Mdm2 by ATM/ATR inhibit p53-Mdm2 interaction and are associated with increased ubiquitination and proteolytic degradation of Mdm2, and increased stability of p53 (Bode and Dong, 2004; Chehab et al., 2000; Maya et al., 2001). Phosphorylation and stabilization of p53 are also associated with increased transcriptional activity and engagement of the p53-associated gene expression programs that facilitate cell cycle arrest and DNA repair (or in some cases, apoptosis) (Appella and Anderson, 2001; Bode and Dong, 2004).

Following completion of damage repair, there must be mechanisms to restore the cell to a prestress homeostatic state. A key component of this homeostatic restoration must be a program to reduce p53 activity and levels. This is likely to be achieved in part by phosphatases that dephosphorylate p53 and Mdm2 to allow Mdm2-p53 interaction and p53 degradation. Previously, we have shown that the wild-type p53-induced phosphatase 1 (Wip1) can dephosphorylate p53 at serine 15, a site adjacent to the Mdm2 interaction domain on p53 (Fujimoto et al., 2006; Lu et al., 2005). Moreover, Wip1 can dephosphorylate and inactivate p53 targeting kinases ATM, Chk1, and Chk2 (Fujimoto et al., 2006; Lu et al., 2005; Oliva-Trastoy et al., 2006; Shreeram et al., 2006; Yoda et al., 2006), which phosphorylate p53 at serine 15 (ATM) and serine 20 (Chk1/2) adjacent to or within the Mdm2 interaction site on p53 (Chehab et al., 2000; Hirao et al., 2000; Yu et al., 2002). We have also shown that Wip1 dephosphorylation of p53 and Chk1 are correlated with abrogation of cell cycle checkpoints (Lu et al., 2005).

Wip1 is a serine/threonine phosphatase of the type 2C protein phosphatase family (PP2C) (Fiscella et al., 1997). The type 2C phosphatases are conserved from yeast to humans and are frequently associated with regulation of cellular stress responses (Choi et al., 2000; Fiscella et al., 1997). Wip1 has the typical properties of a type 2C phosphatase in that it is magnesium dependent and insensitive to the phosphatase inhibitor okadaic acid (Fiscella et al., 1997; Mumby and Walter, 1993). Evidence is accumulating that *Wip1* is a human oncogene. Wip1 cooperates with other oncogenes to transform rodent embryonic fibroblasts (Bulavin et al., 2002; Nannenga et al., 2006). The *Wip1* gene is amplified in several human cancer types (Bulavin et al., 2002; Hirasawa et al., 2003; Li et al., 2002; Mendrzyk et al., 2005; Saito-Ohara et al., 2003). In breast cancers with amplified and overexpressed Wip1, the *p53* locus is rarely mutated (Bulavin et al., 2002), suggesting that Wip1 amplification inhibits p53 activity and reduces selection for *p53* mutations during tumor progression. Recently, it has been demonstrated that Wip1 overexpression in the mammary gland accelerates mammary tumorigenesis in the context of ErbB2 overexpression (Demidov et al., 2007). Interestingly, reduction of Wip1 dosage suppresses transformation in rodent fibroblasts (Bulavin et al., 2004). Moreover, *Wip1* null mice display a dramatic reduction in spontaneous and oncogene-induced tumors compared to their wild-type counterparts (Bulavin et al., 2004; Nannenga et al., 2006). Wip1 inactivation was correlated with activation of $p16^{INK4A}$ and p53 (Bulavin et al., 2004). Thus, *Wip1* is likely to be a bona fide oncogene, at least in part through its capacity to suppress p53 activity.

To determine more mechanistically how Wip1 suppresses p53, we show here that Wip1, also known as PPM1D, stabilizes Mdm2 and facilitates its access to p53. Wip1 dephosphorylates Mdm2 at serine 395, a site that is phosphorylated by the ATM damage response kinase (Maya et al., 2001). Wip1 dephosphorylation of Mdm2 inhibits Mdm2 autoubiquitination and results in its stabilization. In turn, dephosphorylated Mdm2 has increased affinity for p53, and p53 ubiquitination and degradation are increased. Thus, Wip1 acts as a molecular gatekeeper in the Mdm2-p53 autoregulatory loop by stabilizing Mdm2 and facilitating Mdm2-mediated proteolytic degradation of p53. This inhibition of p53 by Wip1 may have clinical implications given the potential therapeutic uses of compounds that interfere with Wip1 suppression of p53 activity (Belova et al., 2005; Yamaguchi et al., 2006).

RESULTS

Absence of Wip1 Enhances p53 Transcriptional Regulatory Functions Following Ionizing Radiation

To further examine how p53 is regulated by Wip1, we assessed the steady-state levels of p53 in human U2OS cells expressing wild-type p53 after DNA damage induced by ionizing radiation (IR). Levels of p53 increased within 2 hr and further increased up to 6 hr after radiation in control cells (Figure 1A). Overexpression of Wip1 in U2OS cells via transfection of a Wip1 expression construct reduced p53 levels compared to controls. In contrast, inhibiting Wip1 by transfection of two distinct Wip1 small interfering RNAs (siRNAs) resulted in higher levels of p53 compared to that in control cells (Figure 1A). To assess the effects of Wip1 on p53 transcriptional activity, we transfected a p53 responsive p21 promoter-luciferase construct along with either a Wip1 expression construct, Wip1 siRNA, or an empty vector into U2OS cells and monitored luciferase activity at varying time points before and after IR treatment. p53 transactivation activity was significantly increased in irradiated U2OS cells transfected with Wip1 siRNA and significantly decreased in cells transfected with the Wip1 construct compared to control vector-transfected cells (Figure 1B). We also examined IR-induced p53 and p21 protein levels in $Wip1^{+/+}$ and $Wip1^{-/-}$

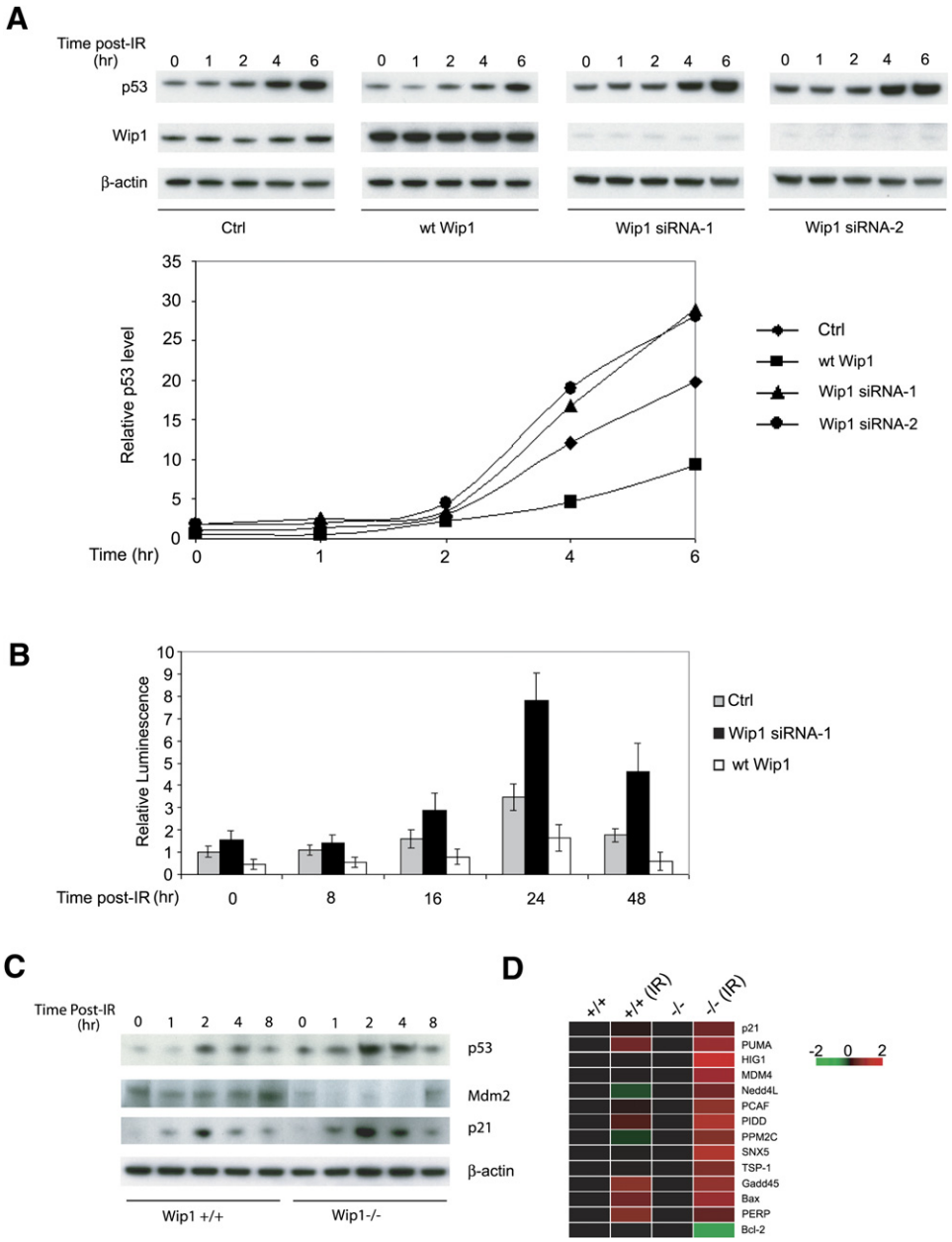

Figure 1. Wip1 Inhibits p53 Levels and Transcription Activity

(A) Steady-state levels of p53 are inhibited by Wip1. Wild-type p53-expressing human U2OS cells were transfected with control scrambled siRNA, wild-type Wip1 expression vector DNA, or Wip1 siRNAs. Twenty-four hours after transfection, cells were irradiated with 5 Gy IR, harvested at various time points, and immunoblotted as previously described (Lu et al., 2005). The graph was generated by normalizing p53 levels to β-actin levels on the western blots using quantitation with a GE Storm 860 fluorescence imager.

(B) The transcriptional activity of p53 is suppressed by Wip1. U2OS cells were transfected with control DNA, wild-type Wip1 expression vector DNA, or Wip1 siRNA-1 together with a p21 promoter-luciferase expression vector and Renilla luciferase control vector DNA. Cells were treated with 5 Gy IR, harvested at indicated time points, lysed, and assayed for luciferase activity. Error bars correspond to standard deviation of the mean.

(C) Absence of Wip1 enhances the abundance and activity of p53 and suppresses Mdm2 protein levels in irradiated MEFs. Primary *Wip1*$^{+/+}$ and *Wip1*$^{-/-}$ MEFs were harvested from littermate embryos as previously described (Choi et al., 2002). These cells were treated with 5 Gy IR, harvested, and immunoblotted as indicated.

(D) p53 target genes have enhanced induction or suppression in response to DNA damage in the absence of Wip1. *Wip1*$^{+/+}$ and *Wip1*$^{-/-}$ MEFs were mock treated or treated with 5 Gy IR. mRNA from each set of cells harvested 4 hr postirradiation was used for gene expression microarray analysis of p53 target genes using the Affymetrix Mouse Genome 430 2.0 Chips. Green on the heat map indicates a reduction of mRNA level, while red indicates an increase. Color intensities correspond to relative signal levels on a logarithmic scale.

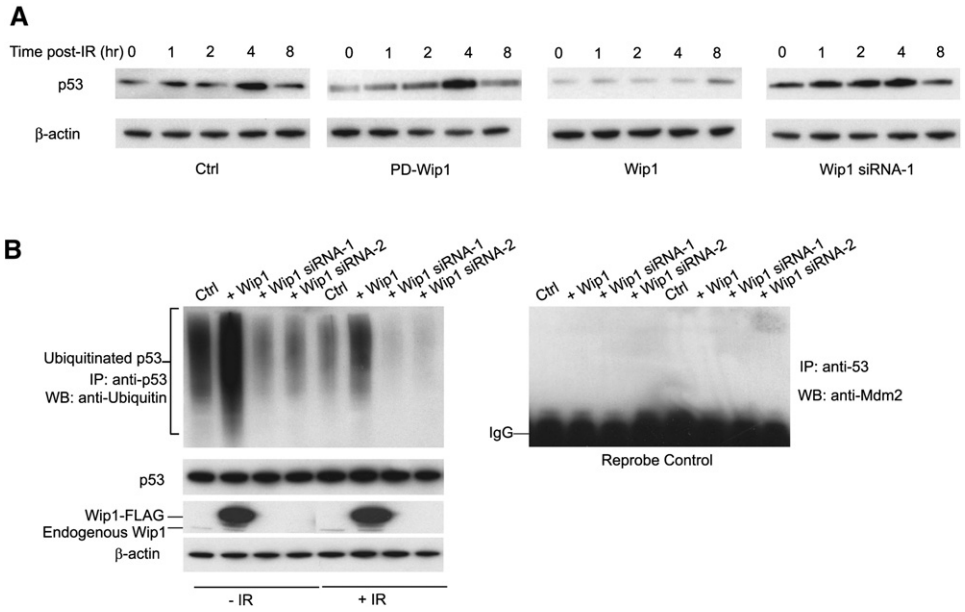

Figure 2. Wip1 Suppresses p53 Accumulation and Promotes Ubiquitination of p53

(A) Wip1 suppresses p53 accumulation regardless of p53 phosphorylation status. Saos-2 cells were transfected with control DNA, wild-type Wip1, or phosphatase-dead (PD) Wip1 (D314A) expression vectors, or Wip1 siRNA-1, together with vector DNA expressing phosphorylation site-deficient mutant p53 (Crook et al., 1994). Transfected cells were treated with IR, harvested, and immunoblotted with p53 or β-actin (loading control) antibody.

(B) Wip1 promotes ubiquitination of p53. p53 null Saos-2 cells were transfected with control scrambled siRNA, Wip1 expression vector DNA, or Wip1 siRNAs, together with the same amount of p53 expression vector DNA. Twenty-four hours after transfection, cells were treated with or without 5 Gy IR and protease inhibitors MG132 and MG102, and harvested 6 hr later. Cell lysates were immunoprecipitated with p53 antibody and immunoblotted with anti-ubiquitin antibody (left panel) or anti-Mdm2 (4B2 and 2A9, Calbiochem) antibody (right panel).

littermate mouse embryonic fibroblasts (MEFs). *Wip1*$^{-/-}$ MEFs exhibited higher levels of p53 and its transcriptional target p21 following IR treatment (Figure 1C), confirming that Wip1 has a suppressive effect on p53 protein levels and transactivation activity. In contrast, despite being a p53 transcriptional target, Mdm2 protein levels were actually decreased in irradiated *Wip1*$^{-/-}$ MEFs, suggesting that Wip1 protein may stabilize Mdm2 protein levels. Assessment of other known p53 targets by gene expression array analysis in irradiated and nonirradiated *Wip1*$^{+/+}$ and *Wip1*$^{-/-}$ MEFs showed a greater p53 transactivation on a number of p53 transactivation targets in *Wip1*$^{-/-}$ MEFs compared to *Wip1*$^{+/+}$ MEFs (Figure 1D). In addition, targets of p53 transcriptional repression (e.g., Bcl-2) were more robustly repressed in *Wip1*$^{-/-}$ MEFs.

Wip1 Destabilization of p53 Is Associated with Increased p53 Ubiquitination

Wip1 directly dephosphorylates p53 at Ser15 (Lu et al., 2005); Wip1 may also indirectly reduce phosphorylation of p53 at Ser20, Ser33, and Ser46 through inactivation of Chk1, Chk2, and p38 MAP kinase (Fujimoto et al., 2006; Lu et al., 2005; Oliva-Trastoy et al., 2006; Takekawa et al., 2000; Yoda et al., 2006). To determine whether suppression of p53 by Wip1 is dependent on p53 phosphorylation status, we used a phosphorylation site-deficient mutant of p53. This mutant p53 had all N-terminal (S6, S9, S15, T18, S20, S33, and S37) and C-terminal (S315, S371, S376, S378, and S392) phosphorylation sites mutated from serine/threonine to alanine (Crook et al., 1994). Wip1 retained its ability to inhibit the levels of mutant p53 in p53 null Saos-2 cells both before and after IR, suggesting that Wip1 must regulate p53 stabilization in additional ways (Figure 2A). To determine how Wip1 influences p53 protein levels, we examined p53 ubiquitination in the presence of increased or decreased Wip1 dosage before and after IR treatment. Overexpressed Wip1 resulted in increased p53 ubiquitination, while reduction of Wip1 via Wip1 siRNA suppressed p53 ubiquitination in both IR-treated and untreated cells (Figure 2B).

Wip1 Interacts with Mdm2 and Dephosphorylates It at Serine 395

p53 protein levels are strongly regulated by Mdm2 (Michael and Oren, 2003). Interestingly, irradiated *Wip1*$^{-/-}$ MEFs exhibited higher p53 protein levels and lower Mdm2 protein levels than irradiated *Wip1*$^{+/+}$ MEFs (Figure 1C). This suggested that Wip1 may play an important role in the p53-Mdm2 autoregulatory loop. The effects of Wip1 on MDM2 activities are likely to be direct, as we showed that endogenous Wip1 binds to endogenous Mdm2 in U2OS cells as measured by reciprocal immunoprecipitation western blot analyses using Wip1 and Mdm2 antibodies (Figure 3A). If U2OS cells are transfected with Wip1 siRNA, the Mdm2-Wip1 interaction is lost due to the absence of Wip1, as expected (Figure 3B). To determine whether Wip1 dephosphorylates Mdm2, we performed in vitro phosphatase assays by incubating purified

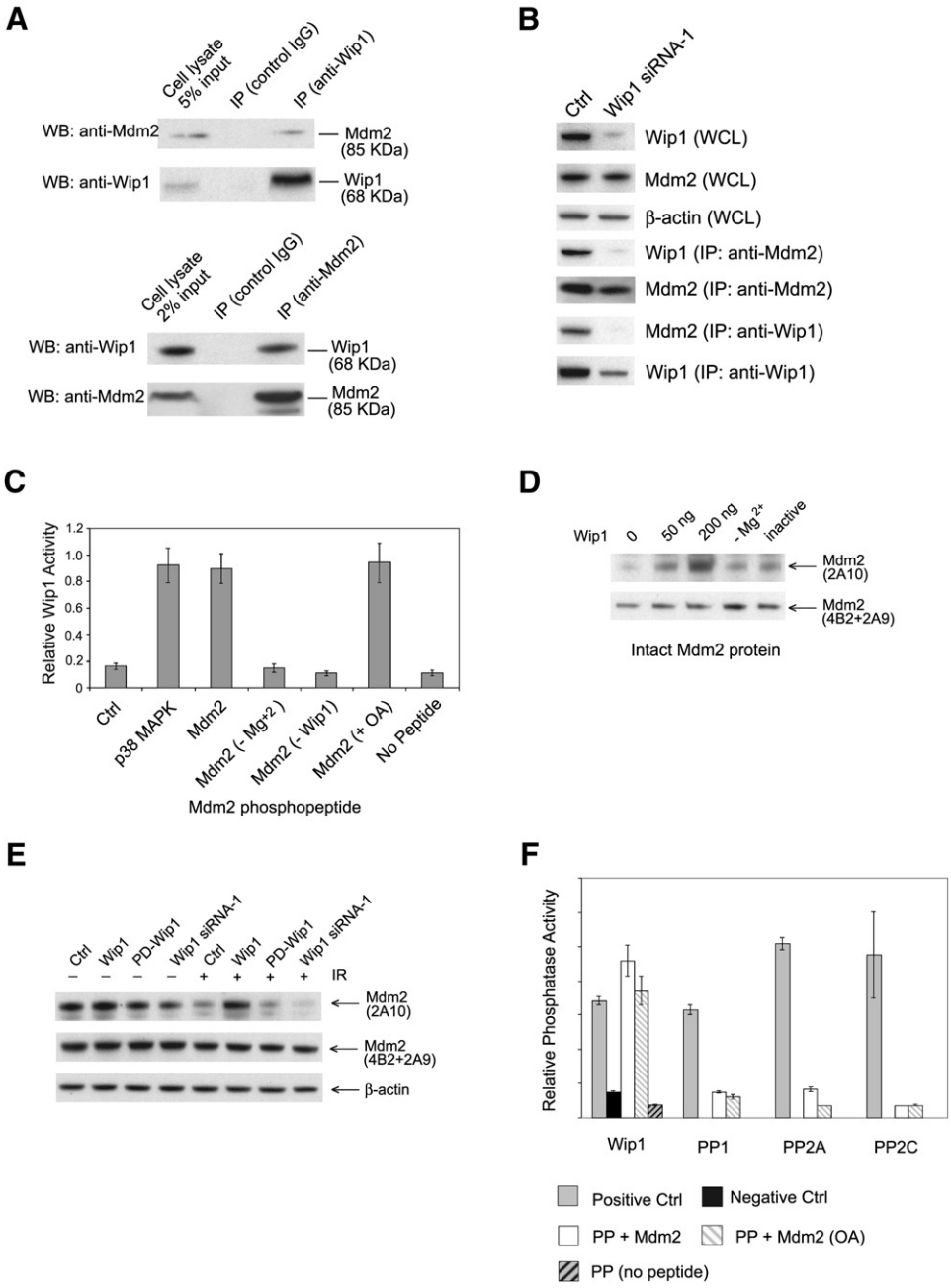

Figure 3. Wip1 Interacts with and Dephosphorylates Mdm2

(A) Endogenous Wip1 interacts with endogenous Mdm2. U2OS cells were lysed and immunoprecipitated with Mdm2 (Calbiochem, cat. no. OP144 and OP145) or Wip1 (Trevigen, Cat. no. 2380-MC-100) antibody and immunoblotted with Wip1 or Mdm2 antibody as indicated.

(B) U2OS cells were transfected with control scrambled siRNA or Wip1 siRNA-1, lysed and immunoprecipitated with the above Mdm2 or Wip1 antibody, and immunoblotted with Wip1 or Mdm2 antibody as indicated. Whole-cell lysates (WCL) were also immunoblotted as indicated.

(C) Wip1 dephosphorylates Mdm2 peptides containing phosphoserine 395. FLAG-Wip1 proteins were purified from 293HEK cells overexpressing FLAG-Wip1 by affinity columns and incubated with an Mdm2 phosphoserine 395 peptide. A known Wip1 target phosphopeptide (pT180) from p38 MAP kinase was utilized as a positive control. Free phosphate released by dephosphorylation was bound by molybdate and measured by O.D. absorbance at 562 nm as previously described (Lu et al., 2004). Wip1 activity is magnesium dependent and is insensitive to the PP2A inhibitor okadaic acid (OA). Error bars correspond to standard deviation of the mean.

(D) Wip1 dephosphorylates intact Mdm2 protein. Intact Mdm2 proteins were immunopurified from U2OS cells treated with IR and incubated with indicated amounts of purified Wip1. Dephosphorylation of Mdm2 was measured by immunoblotting with an Mdm2 antibody (2A10) that only recognizes unphosphorylated Mdm2 at serine 395.

Wip1 with an Mdm2-derived phosphoserine 395 peptide (Figure 3C) or intact immunopurified Mdm2 (Figure 3D). The Mdm2 phosphopeptide was dephosphorylated by Wip1 in a dose-dependent manner at serine 395, a site that is phosphorylated by the ATM kinase (Maya et al., 2001) (Figure 3C). This Wip1 activity was magnesium dependent and okadaic acid insensitive, consistent with the known properties of Wip1, a type 2C phosphatase (Fiscella et al., 1997) (Figures 3C and 3D). A monoclonal antibody (2A10) that recognizes a nonphosphorylated serine 395 epitope of Mdm2 (Maya et al., 2001) was used to analyze the phosphorylation status of Mdm2 in vitro with purified Wip1 or in vivo in cells with overexpression or knockdown of Wip1 (Figures 2D and 2E). Phosphorylation of Mdm2 at serine 395 was inhibited by Wip1 in vitro or by Wip1 overexpression in vivo and was enhanced by Wip1 siRNA transfection following IR treatment of cells in vivo (Figure 3E). Three other serine/threonine protein phosphatases were tested in in vitro phosphatase assays with the Mdm2 serine 395 phosphopeptide, including PP2A, which has been shown to dephosphorylate Mdm2 at threonine 216 (Okamoto et al., 2002). These phosphatases (including the closely related PP2Cα, which can augment p53 activity [Ofek et al., 2003]) showed no appreciable enzyme activity on the Mdm2 serine 395 phosphopeptide (Figure 3F).

Wip1 Enhances p53-Mdm2 Interaction and Mdm2 Stability

Phosphorylation on p53 (ser15, thr18, ser20) and Mdm2 (ser395) inhibits the p53-Mdm2 interaction, suggesting that Wip1 may facilitate this interaction through reduction of phosphorylation (Bode and Dong, 2004; Moll and Petrenko, 2003). Indeed, Wip1 overexpression enhanced the p53-Mdm2 interaction in IR-treated, p53-transfected p53 null Saos-2 cells, leading to a reduced steady-state level of p53 (and p53 serine 15 phosphorylation) after IR treatment (Figure 4).

To assess Wip1 effects on Mdm2 protein levels, we examined p53 null Saos-2 cells and p53-containing HEK293 and U2OS cells transfected with Wip1 expression constructs or empty vectors. Wip1 attenuated the IR-associated decrease in Mdm2 levels in all three cell types (Figure 5A). We measured the half-life of wild-type and phosphorylation mutant Mdm2 proteins in $p53^{-/-}Mdm2^{-/-}$ MEFs that simplify the analysis of transfected Mdm2 by eliminating endogenous Mdm2. As measured by pulse-chase analysis, the mean half-life of wild-type Mdm2 after IR treatment was about 21 min, which extended to 38 min in the presence of overexpressed Wip1 (Figure 5B). An Mdm2 mutation at Ser395 (S395A) that mimics a nonphosphorylated form of Mdm2 resulted in enhanced Mdm2 stability, which was not significantly increased in the presence of Wip1 overexpression (Figure 5B). This suggests that the primary effect of Wip1 on Mdm2 stability is mediated by its dephosphorylation of serine 395. This is confirmed by the Mdm2 S395D mutant, which mimics a phosphorylated form of Mdm2, since the mutant had a much shorter half-life of about 8 min that was not significantly affected by Wip1 overexpression (Figure 5B).

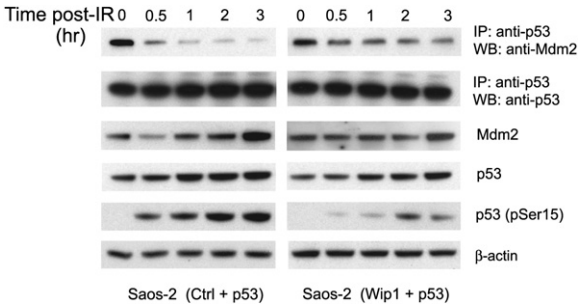

Figure 4. Wip1 Enhances the p53-Mdm2 Interaction

Saos-2 cells were transfected with p53 expression vector DNA and control DNA or Wip1 expression vector DNA. Twenty-four hours after transfection, cells were treated with 5 Gy IR, harvested, and lysed at indicated times. The p53-Mdm2 interaction was analyzed by immunoprecipitation-western blotting as indicated.

Since ATM phosphorylates Mdm2 at serine 395 (Maya et al., 2001), we tested whether Wip1 effects on Mdm2 stability are ATM dependent. An ATM-deficient human cell line (GM09607) was used to determine whether increased levels of Wip1 promote Mdm2 accumulation in the absence of functional ATM signaling. Mdm2 remained relatively stable in IR-treated A-T cells regardless of Wip1 levels (Figure 5C). When ATM was reintroduced into these cells, Mdm2 became more unstable following IR treatment. Addition of Wip1 helped to stabilize Mdm2 in the ATM-containing cells (Figure 5C), again indicating that Wip1 stabilizes Mdm2 by reversing the destabilizing effects of ATM phosphorylation. To confirm that the effects of Wip1 on p53 stability are largely Mdm2 dependent, we transfected $p53^{-/-}Mdm2^{-/-}$ MEFs with exogenous p53 expression vectors with or without Wip1 expression constructs. Overexpression of Wip1 had no detectable effect on p53 accumulation in the $p53^{-/-}Mdm2^{-/-}$ MEFs with or without IR (Figure 5D). In contrast, introduction of Wip1 into wild-type MEFs inhibited p53 accumulation.

Wip1 May Augment Mdm2 Stability by Suppressing Mdm2 Self-Interaction and Autoubiquitination and by Enhancing Mdm2-HAUSP Interactions

Mdm2 stability is regulated by autoubiquitination following self-interaction of Mdm2 monomers (Meek and

(E) Wip1 dephosphorylates Mdm2 in cells. U2OS cells were transfected with control DNA, Wip1 or phosphatase-dead Wip1 expression vector DNA, or Wip1 siRNA-1, treated with 5 Gy IR, harvested 4 hr later, and immunoblotted with serine 395 phosphorylation-sensitive Mdm2 antibody 2A10 (top panel) or phosphorylation-insensitive Mdm2 antibodies 4B2 and 2A9 (middle panel).

(F) Wip1, but not other serine/threonine phosphatases, dephosphorylates Mdm2 at serine 395. Wip1, PP1, PP2A, and PP2Cα protein phosphatases (PP) were incubated with their specific positive control phosphopeptides, or Mdm2 serine 395 phosphopeptide, or no peptide. The phosphatase activity was measured as in (C). Error bars in (C) and (F) show the standard deviations of mean values.

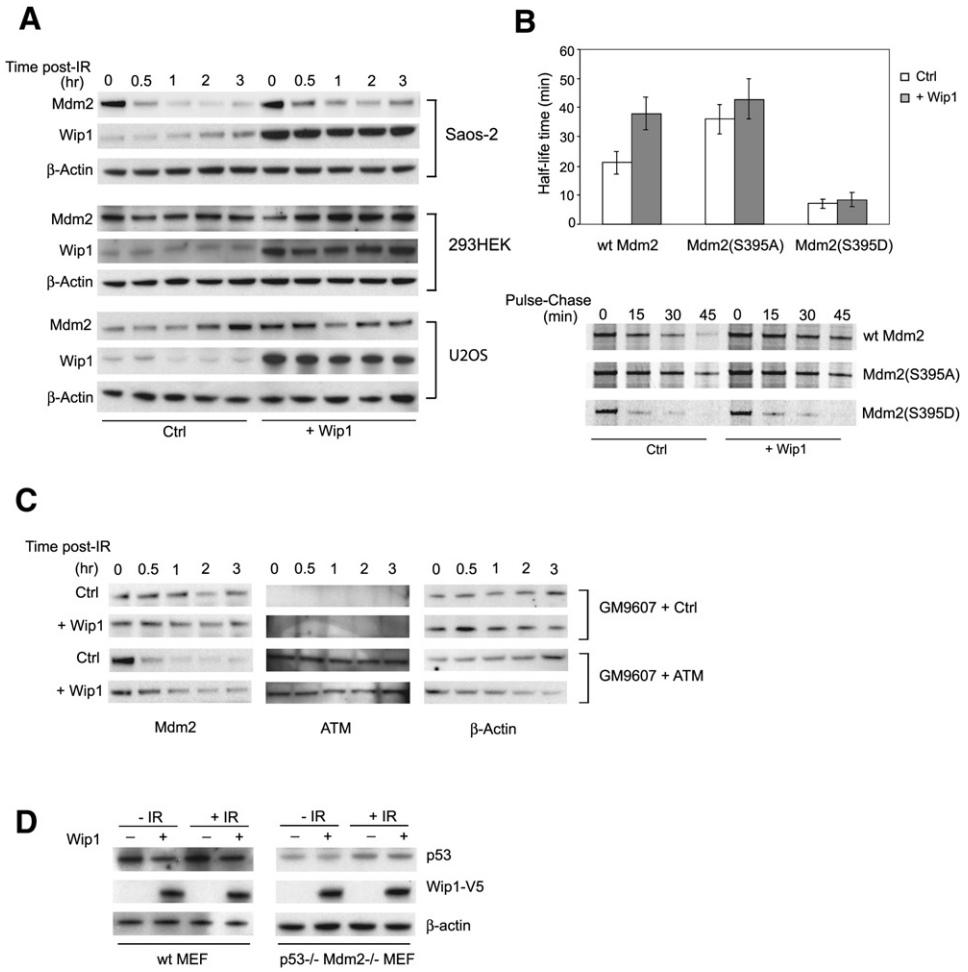

Figure 5. Wip1 Stabilizes Mdm2 in an ATM-Dependent Manner

(A) Mdm2 levels are enhanced by overexpression of Wip1 in either p53 null or p53-expressing cells. Saos-2, 293HEK, and U2OS cells were transfected with control DNA or Wip1 expression vector DNA. Twenty-four hours after transfection, cells were treated with 5 Gy IR, harvested and immunoblotted.

(B) Mdm2 is stabilized by Wip1. $p53^{-/-}Mdm2^{-/-}$ MEFs were transfected with wild-type Mdm2 or serine 395 mutant Mdm2 expression vector DNA together with Wip1 expression vector DNA or control DNA. Twenty-four hours after transfection, cells were treated with 5 Gy IR. Cells were pulse labeled with ^{35}S-L-methionine and ^{35}S-L-cysteine for 1 hr, harvested at the indicated time points after labeling, and cell lysates were immunoprecipitated with Mdm2 antibodies. The levels of Mdm2 at each time point were quantitated by phosphorimager for Mdm2 bands on SDS-PAGE gels, and Mdm2 half-life was calculated (from two separate experiments) for the graph in the upper panel. Error bars correspond to standard deviation of the mean.

(C) Wip1 stabilizes Mdm2 only in the presence of ATM. A-T cells (GM09607) were transfected with control DNA or Wip1 expression vector DNA, together with ATM expression vector DNA or control DNA. Twenty-four hours after transfection, cells were treated with 5 Gy IR, harvested, and immunoblotted as indicated.

(D) The accumulation of p53 is regulated by Wip1 primarily through Mdm2. Wild-type or $p53^{-/-}Mdm2^{-/-}$ MEFs were transfected with V5 epitope-tagged Wip1 expression vector DNA or control DNA, together with p53 expression vector DNA. Twenty-four hours after transfection, cells were treated with or without 5 Gy IR, and lysed 2 hr after irradiation and immunoblotted as indicated.

Knippschild, 2003). We tested whether Wip1 regulates Mdm2 stability by modulating Mdm2 self-interaction and ubiquitination. To quantitate self-interaction of Mdm2, expression vectors encoding HA- and FLAG-tagged Mdm2 were cotransfected into HEK293 cells that inducibly express Wip1 in the presence of doxycycline. Increased Wip1 expression reduced the interaction between HA-Mdm2 and FLAG-Mdm2 before and after IR treatment (Figure 6A). We then examined the effects of altered Wip1 levels on Mdm2 ubiquitination. Overexpression of Wip1 lowered Mdm2 ubiquitination while reduction of Wip1 levels through Wip1 siRNA transfection enhanced Mdm2 ubiquitination compared to empty vector-transfected control cells (Figure 6B). Thus, Wip1 promotes Mdm2 stabilization through inhibition of Mdm2 autoubiquitination.

To assess the effects of Wip1 on Mdm2 deubiquitination, we examined binding of Mdm2 to HAUSP in U2OS

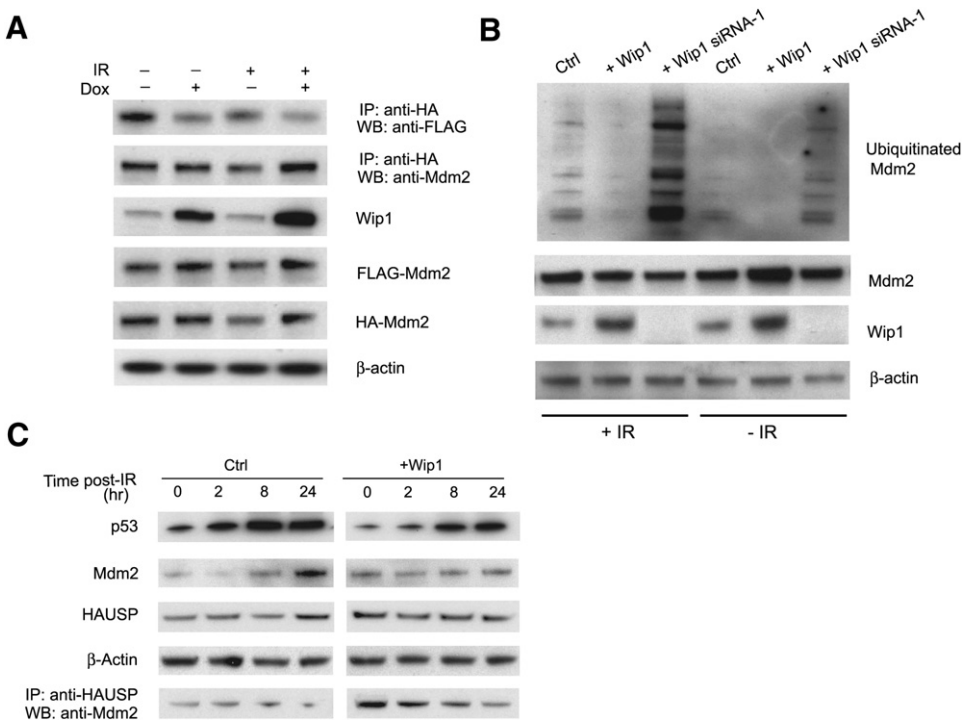

Figure 6. Wip1 Inhibits Ubiquitination of Mdm2

(A) Wip1 diminishes Mdm2 self-interaction. 293HEK cells that inducibly express Wip1 in the presence of doxycycline were transfected with equal amounts of HA-Mdm2 and FLAG-Mdm2 expression vector DNA, treated with or without 5 Gy IR, and harvested 2 hr later. The Mdm2 self-interaction was analyzed by immunoprecipitation and immunoblotting as indicated.

(B) Ubiquitination of Mdm2 is inhibited by Wip1. The same 293HEK cells as above were transfected with HA-ubiquitin expression vector, together with control DNA, or Wip1 expression vector DNA or Wip1 siRNA-1. Transfected cells were treated with or without 5 Gy IR and with protease inhibitor MG132, and harvested 2 hr after IR. Cell lysates were immunoprecipitated with anti-HA antibody and immunoblotted by anti-Mdm2 antibody.

(C) Wip1 enhances the HAUSP-Mdm2 interaction. U2OS cells were transfected with or without Wip1 expression vector DNA, treated with IR, harvested, and immunoblotted as indicated.

cells. HAUSP enhances Mdm2 stability by removing ubiquitin moieties from Mdm2 (Li et al., 2004; Meulmeester et al., 2005). While the levels of HAUSP remained constant before and after ionizing radiation, the relative amounts of Mdm2 bound to HAUSP were increased by overexpressed Wip1 (Figure 6C). This result suggests that Wip1 enhances binding of HAUSP to Mdm2 and contributes to Mdm2 stability by facilitating its deubiquitination.

ATM-Independent Effects of Wip1 on Mdm2 Stability

In Figure 5C, when ATM-deficient human A-T cells were treated with ionizing radiation, alteration of Wip1 levels had little effect on apparent Mdm2 levels. When ATM was restored in the A-T cells, increased Wip1 again stabilized Mdm2. Such results suggested that Wip1 effects on Mdm2 stability were largely ATM dependent. To determine whether Wip1 is solely ATM dependent or can exhibit ATM independence, we assessed Wip1 effects on Mdm2 stability in the absence of ATM in two separate contexts. First, we examined the effects of increased Wip1 levels on Mdm2 stability in UV-irradiated A-T cells. UV irradiation primarily activates the ATR pathway rather than ATM, and we hypothesized that ATR phosphorylation of Mdm2 serine 395 might compensate for the absence of ATM. In fact, overexpression of Wip1 did increase Mdm2 stability after UV irradiation of A-T cells (Figure 7A). In addition, phosphorylation of Mdm2 serine 395 was lower in the UV irradiated A-T cells with extra Wip1, as measured by the 2A10 serine 395 epitope-specific antibody, suggesting that ATR might be phosphorylating this site and that Wip1 can suppress this phosphorylation even in the absence of ATM.

A second approach to assess ATM independence of Wip1 was performed by examining Mdm2 stability in mouse tissues lacking ATM in the presence and absence of Wip1. We crossed ATM-deficient mice to Wip1-deficient mice and obtained $ATM^{-/-}$ $Wip1^{-/-}$ F2 offspring after two generations of crosses. $ATM^{+/+}$ $Wip1^{+/+}$, $ATM^{+/+}$ $Wip1^{-/-}$, $ATM^{-/-}$ $Wip1^{+/+}$, and $ATM^{-/-}$ $Wip1^{-/-}$ mice were then irradiated with 8 Gy ionizing radiation, and tissues were harvested 16 hr later. Protein lysates from spleens were western blot probed with antibodies to p53 protein, p53 serine 18 (the ATM/ATR phosphorylated mouse p53 site equivalent to serine 15 on human p53), and Mdm2 protein. Irradiated $Wip1^{-/-}$ mice exhibited increased levels of p53 protein and p53 serine 18 phosphorylation compared to wild-type mice (Figure 7B, lanes 5–8). Moreover, Mdm2

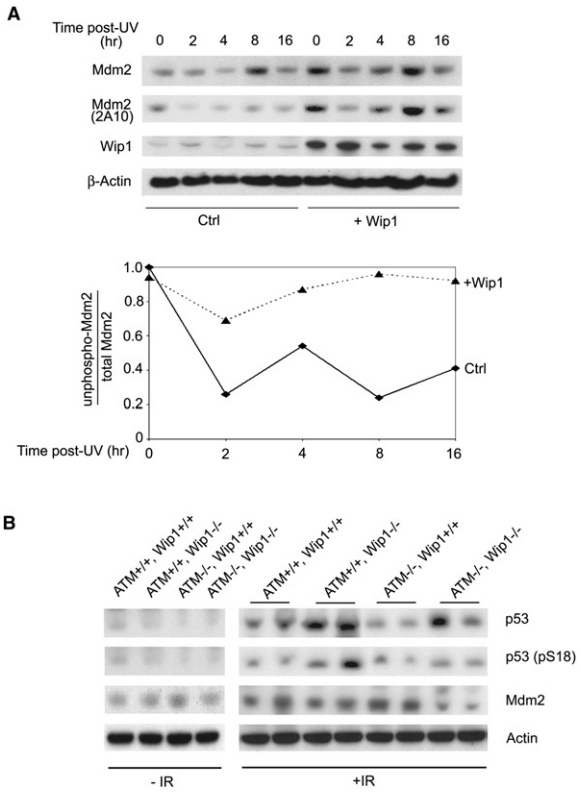

Figure 7. ATM-Independent Effects of Wip1 on Mdm2 Protein Levels

(A) Wip increases Mdm2 protein levels in UV-treated ATM-deficient cells. GM09607 A-T cells were transfected with empty vector or Wip1 expression vector. Twenty-four hours after transfection, the GM09607 cells were UV irradiated (60 J/m^2). Cell lysates were harvested at the indicated times post-V treatment, and western blots were probed with the indicated antibodies. The Mdm2 2A10 antibody is specific for the nonphosphorylated S395 form of Mdm2. The lower graph shows the densitometric quantitation of relative unphosphorylated Mdm2 in empty vector or Wip1 vector-transfected cells.

(B) Absence of Wip1 in ATM-deficient mice suppresses Mdm2 protein levels after ionizing radiation treatment. Adult (8–10 weeks) wild-type (*ATM*$^{+/+}$ *Wip1*$^{+/+}$) mice, Wip1 null (*ATM*$^{+/+}$ *Wip1*$^{-/-}$) mice, ATM null (*ATM*$^{-/-}$ *Wip1*$^{+/+}$) mice, and ATM/Wip1 double null (*ATM*$^{-/-}$ *Wip1*$^{-/-}$) mice were treated with 8 Gy ionizing radiation and euthanized 16 hr later. Spleen protein lysates were prepared and western blot probed with the indicated antibodies. Two animals of each ATM/Wip1 genotype were irradiated, and *Wip1*$^{-/-}$ mice consistently show reduced Mdm2 protein levels compared to their *Wip1*$^{+/+}$ counterparts in the presence or absence of ATM. Shown at the left are spleen lysates from nonirradiated mice, indicating little activation of p53 or Mdm2.

protein levels were modestly decreased in the Wip1 null mice compared to wild-type mice. In the absence of ATM (Figure 7B, lanes 9 and 10), levels of p53 protein and serine 18 phosphorylation were decreased and Mdm2 levels increased. However, when both ATM and Wip1 were absent (Figure 7B, lanes 11 and 12), p53 levels were increased and Mdm2 levels were decreased relative to ATM-deficient mice. This result is consistent with an ATM-independent role of Wip1 in enhancement of Mdm2 stability and suppression of p53 stability.

DISCUSSION

The p53 protein is a key integrator of the DNA damage response initiated by sensor kinases such as ATM and ATR (Shiloh, 2003). Following DNA damage, ATM and ATR phosphorylate p53 either directly or indirectly through intermediates such as Chk1 and Chk2 kinases (Toledo and Wahl, 2006). Phosphorylation of p53 near its N terminus is associated with activation of p53 in part through stabilization. In conjunction with p53 phosphorylation, damage-activated ATM also phosphorylates serine 395 on the E3 ubiquitin ligase Mdm2 (Maya et al., 2001). This particular phosphorylation facilitates Mdm2 proteasomal degradation and reduces overall Mdm2 protein levels (Maya et al., 2001; Stommel and Wahl, 2005). Thus, not only is less Mdm2 available, but phosphorylation of p53 in the p53-Mdm2 binding domain likely prevents p53 and Mdm2 interaction (Bode and Dong, 2004). Since Mdm2 binding to p53 promotes p53 ubiquitination and degradation, prevention of this binding is a major factor in stabilizing p53.

Stabilized and activated p53 transactivates a large battery of genes that can mediate DNA repair or arrest the cell at multiple stages of the cell cycle (if apoptosis programs are not engaged) (Figure 8). Assuming that p53 successfully facilitates cell cycle arrest and DNA repair, a mechanism to return the cell to a predamage state is required. Critical to returning the repaired cell to a homeostatic state is the reduction of p53 levels. Central to this p53 homeostatic response is the accumulation of Mdm2 following transactivation by p53. Eventually, accumulated Mdm2 may bind to p53 and promote its degradation. This has been the central paradigm of the p53-Mdm2 negative feedback regulatory loop. However, this simple autoregulatory loop does not take into account the possibility that p53 and Mdm2 may remain phosphorylated for some time following DNA damage. One way to expedite p53 degradation after successful DNA repair would rely on dephosphorylation of those sites on p53 and Mdm2 that inhibit p53-Mdm2 interactions.

The findings reported here indicate that the serine/threonine phosphatase Wip1 plays an integral role in the p53-Mdm2 negative feedback regulatory loop. The effects of Wip1 on Mdm2 are multiple and include (1) dephosphorylation of Mdm2 at serine 395, (2) stabilization of Mdm2 through decreased Mdm2 self-interaction and self-ubiquitination, (3) stabilization of Mdm2 through facilitation of HAUSP binding and Mdm2 deubiquitination, (4) facilitation of Mdm2 binding to p53, and (5) stimulation of Mdm2-mediated p53 ubiquitination and proteolytic degradation (Figure 8). By dephosphorylating Mdm2 at serine 395, Wip1 reverses the effects of the ATM and ATR kinases that enhance p53 stability and mediate the damage response. Consistent with this scenario is the fact that, like Mdm2, Wip1 is a p53 transcriptional target. The kinetics of p53-mediated Wip1 induction are somewhat delayed compared to that of p21 (compare Figure 1A and Figure 1C). Such a delay in Wip1 expression would allow p53-induced cell cycle arrest and DNA repair to proceed without premature interference.

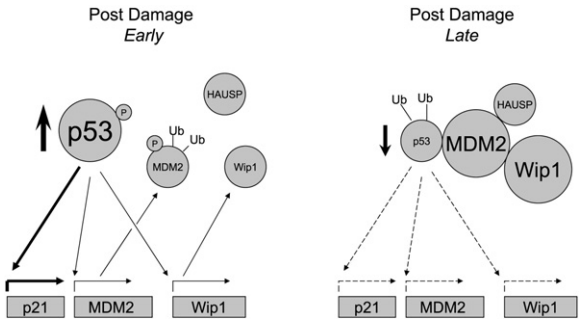

Figure 8. Wip1 Plays Multiple Roles in the p53-Mdm2 Autoregulatory Loop

At left, early after DNA damage p53 levels are stabilized as a result of p53 and Mdm2 phosphorylation by ATM. Phosphorylation of Mdm2 destabilizes it and results in self-ubiquitination and degradation. Stabilized p53 transactivates a number of genes including *p21*, *Mdm2*, and *Wip1*. At right, at later time points after damage, Mdm2 and Wip1 protein levels increase, and Wip1 dephosphorylates p53 and Mdm2, stabilizing Mdm2 in part through interactions with the HAUSP deubiquitinase. Dephosphorylated p53 and Mdm2 more readily bind, initiating the ubiquitination-mediated proteolysis of p53. This reduces p53 protein levels and returns the cell to a prestress-like state.

By dephosphorylating Mdm2 and p53, Wip1 may act as a molecular gatekeeper that allows Mdm2 to bind more efficiently to p53. This promotes p53 ubiquitination and degradation. Without Wip1, the p53 damage response is likely to be enhanced and extended due in part to inefficient p53-Mdm2 binding. This is seen in Figure 1, where Wip1 siRNA treatment or targeted deletion of Wip1 in cells results in increased p53 protein levels and activation of p53 target genes following radiation compared to cells with normal Wip1 activity. Moreover, in Figure 7, we show that tissues of Wip1 null mice treated with ionizing radiation exhibit increased p53 stabilization and p53 serine 18 phosphorylation in comparison to wild-type mice. This is correlated with enhanced cancer resistance observed in the Wip1-deficient animals (Nannenga et al., 2006).

Is dephosphorylation of Mdm2 at serine 395 the primary mechanism by which Wip1 enhances stability of Mdm2? While we believe this is the case, an alternative possibility is that Wip1 dephosphorylation of ATM at serine 1981, as recently demonstrated (Shreeram et al., 2006), will have a similar effect in inhibiting ATM kinase function and leaving Mdm2 unphosphorylated at serine 395. If this latter scenario is dominant, Wip1 effects on Mdm2 stability should be ATM dependent. In the absence of ATM, increased Wip1 would have little or no effect on the unphosphorylated serine 395, and Mdm2 would be more stable with or without Wip1. When ionizing radiation, which rapidly activates ATM, is applied to ATM-deficient cells, Mdm2 stability is in fact Wip1 independent (Figure 5C). However, experiments presented in Figure 7A showed that, in the absence of ATM, ultraviolet radiation, which primarily activates ATR, results in Wip1-dependent Mdm2 stability. Moreover, experiments in Figure 7B show ionizing radiation applied to ATM null mice produces Wip1-dependent Mdm2 alterations in stability in vivo, indicating that Wip1 is ATM independent in multiple contexts. These latter experiments likely entailed the activation of other sensor kinases such as ATR and DNA-PK_{cs}, which can compensate for ATM absence by phosphorylating many ATM targets. However, even in the presence of activated ATM, it seems likely that Wip1 dephosphorylation of both ATM serine 1981 and Mdm2 serine 395 contributes to Mdm2 stabilization. We conclude that a major component of Wip1 effects on Mdm2 stability is a result of direct dephosphorylation of Mdm2 at serine 395, reversing the effects of phosphorylation at this site by ATM and other kinases such as ATR.

In addition to the effects of Wip1 on p53 activity via Mdm2, Wip1 may suppress p53 activities by other mechanisms. Wip1 dephosphorylates and reduces the activities of the upstream p53 targeting kinases p38 MAP kinase (phosphorylates p53 serines 33 and 46), ATM (phosphorylates p53 serine 15), and Chk1 and Chk2 (p53 serine 20 phosphorylation) (Fujimoto et al., 2006; Lu et al., 2005; Oliva-Trastoy et al., 2006; Shreeram et al., 2006; Takekawa et al., 2000; Yoda et al., 2006). Dephosphorylation at each of these sites is likely to reduce p53 activity. For example, phosphorylation of p53 serines 33 and 46 by p38 MAP kinase promotes p53 apoptotic function (Sanchez-Prieto et al., 2000). That serine 15 phosphorylation by ATM plays a significant role in p53 function is underlined by the finding that mutation of serine 18 to a nonphosphorylatable alanine results in mice with decreased damage-induced apoptotic function and an accelerated rate of tumor formation (Sluss et al., 2004; S.N.J., unpublished data). In addition to inhibiting ATM phosphorylation of p53 serine 15, Wip1 dephosphorylates p53 at this site (Lu et al., 2005).

The ability of Wip1 to suppress p53 activity through different mechanisms makes it an obvious oncogene candidate, analogous in some ways to Mdm2, which appears to be oncogenic largely due to inhibition of p53 (Bond et al., 2005; Momand et al., 1998). Indeed, Wip1 can cooperate with Ras and other oncogenes to transform rodent primary fibroblasts (Bulavin et al., 2002; Li et al., 2002; Nannenga et al., 2006). In contrast, Wip1 null MEFs are resistant to oncogene-induced transformation (Bulavin et al., 2004). Moreover, overexpression of Wip1 in mouse mammary gland accelerates mammary tumorigenesis initiated by the ErbB2 oncogene (Demidov et al., 2007), while Wip1 null mice are resistant to spontaneous and oncogene-induced cancers (Bulavin et al., 2004; Nannenga et al., 2006). Finally, some human cancer types exhibit amplification and overexpression of Wip1 (Bulavin et al., 2002; Hirasawa et al., 2003; Li et al., 2002; Mendrzyk et al., 2005; Saito-Ohara et al., 2003). That Wip1 is oncogenic in part through its ability to suppress p53 is suggested by the virtual absence of p53 mutations in breast tumors with amplified Wip1 (Bulavin et al., 2002). Thus, Wip1 is unusual in being a serine/threonine phosphatase that behaves as an oncogene.

In summary, we have demonstrated here that Wip1 plays an important role in the p53-Mdm2 autoregulatory loop. It is upregulated in a p53-dependent manner following DNA damage and it acts to stabilize Mdm2 by dephosphorylating it at serine 395, thus reversing the destabilizing

effects of ATM and ATR phosphorylation at that site. In turn, dephosphorylated Mdm2 is stabilized and more capable of binding to p53 (also dephosphorylated by Wip1) and mediating its ubiquitination and proteasomal degradation. The above scenario provides further mechanistic insights into Wip1 oncogenic function that supplements previous studies implicating Wip1 in suppression of p38 MAP kinase signaling, ATM/ATR signaling, $p16^{INK4A}$ function, cell cycle checkpoints, and DNA repair (Bulavin et al., 2004; Demidov et al., 2007; Lu et al., 2004, 2005). Thus, interruption of Wip1 function in cancers could be an effective therapeutic approach that merits further study.

EXPERIMENTAL PROCEDURES

Cell Lines and Cell Culture

U2OS (p53 wild-type) and Saos-2 (p53 null) cell lines are human osteosarcoma lines that were obtained from the American Type Culture Collection (ATCC). Primary *Wip1*$^{+/+}$, *Wip1*$^{-/-}$, and *p53*$^{-/-}$*Mdm2*$^{-/-}$ MEFs were harvested and cultured as previously described (Choi et al., 2002; Jones et al., 1996). The A-T cell line GM09607 was obtained from Coriell Cell Repositories. 293 HEK Tet-on cells were obtained from BD Biosciences (BD Biosciences, catalog #630903). To obtain cells stably expressing Wip1, FLAG-tagged Wip1 cDNA was inserted into the BamH1 site in pRevTRE vector (BD Biosciences, catalog #631002). Together with retroviral packaging plasmids pVSVG and pHit60 (provided by R. Sutton), pRexTRE-Wip1 was transfected into 293T cells to generate retroviral vectors containing FLAG-Wip1. 293 HEK Tet-on cells were infected with the above retrovirus, then screened with 400 μg/ml hygromycin. Twelve hygromycin-resistant positive colonies were isolated, amplified, and checked for inducible expression of Flag-Wip1 protein following addition of 5.0 μg/ml doxycycline (BD Biosciences, catalog #631311) individually. Clonal lines with high levels of inducible Wip1 expression and low basal levels of FLAG-Wip1 were used for the experiments described in this paper.

Mice and Mouse Embryo Fibroblasts

ATM-deficient mice were a generous gift from Dr. Ben Zhu and have been previously described (Sekiguchi et al., 2001). The ATM-deficient mice were crossed to Wip1 mice previously generated by our laboratory (Choi et al., 2002), and *ATM*$^{-/-}$ *Wip1*$^{-/-}$ F2 offspring were obtained. For the experiments in Figure 7B, two 8- to 10-week-old male mice of each ATM/Wip1 genotype (*ATM*$^{+/+}$ *Wip1*$^{+/+}$, *ATM*$^{+/+}$ *Wip1*$^{-/-}$, *ATM*$^{-/-}$ *Wip1*$^{+/+}$, and *ATM*$^{-/-}$ *Wip1*$^{-/-}$) were irradiated with 8 Gy ionizing radiation and were euthanized 16 hr later. For mouse embryo fibroblast studies using *Wip1*$^{-/-}$ MEFs, *Wip1*$^{+/-}$ mice were crossed and MEFs prepared as described previously (Choi et al., 2002). *p53*$^{-/-}$*Mdm2*$^{-/-}$ MEFs were prepared in a similar manner from *p53*$^{-/-}$*Mdm2*$^{-/-}$ parental crosses (Jones et al., 1996). All experiments utilizing mice were performed in accordance with relevant regulatory standards regarding animal research and were approved by the Baylor College of Medicine Institutional Animal Care and Use Committee.

Plasmid Constructs and siRNAs

Wild-type Wip1 plasmids expressing mouse and human Wip1 used in these experiments have been previously described (Lu et al., 2004). The phosphatase-dead Wip1 point mutant D314A is catalytically inactive and was obtained from Dr. Y. Minami (Yoda et al., 2006). The p21-luciferase construct was obtained from Dr. G. Lozano. The vectors expressing wild-type Mdm2, Mdm2 (S395A and S395D) were previously described (Maya et al., 2001). The sequences of the Wip1 siRNAs are GGCUUUCUCGCUUGUCACC (siRNA-1) and UUGGCCUUGUGCC UACUAA (siRNA-2). Control scrambled siRNA was purchased from Dharmacon (catalog #D-001210-01-05).

Cell Transfection with Plasmid DNA or siRNA

Cells were transfected with plasmid DNA by Lipofectamine and Plus reagents (for transformed cell lines, Invitrogen, catalog #18324-012 and #11514-015) or Lipofectamine 2000 reagent (for MEFs, Invitrogen, catalog #11668-019). Oligofectamine reagents (Invitrogen, catalog #12252-011) were utilized to transfect cells with siRNAs. Transfection experiments were performed following the instruction manuals provided with reagents.

Luciferase Assays

U2OS cells were cotransfected with p21-Luciferease DNA, Renilla luciferase DNA, and Wip1 expression vector DNA or Wip1 siRNA. Cells were harvested at various time points and lysed. Luciferase activity was measured using a Turner TD-20e luminometer and normalized to renilla luciferase according to the instructions provided with the dual-luciferase assay kit (Promega).

Gene Expression Microarray Analysis

RNA was extracted from 60 mm dishes of irradiated or nonirradiated *Wip1*$^{+/+}$ or *Wip1*$^{-/-}$ MEFs 4 hr after 5 Gy of radiation with RNeasy Mini Kit (QIAGEN). Following quality check of the RNA, microarray analysis was performed at Baylor Microarray Core Facility (http://www.bcm.edu/mcfweb/) with Affymetrix Mouse Genome 430 2.0 Chips. Microarray data were analyzed with Genesifter software (http://www.genesifter.net/). The raw data for the microarray analyses have been deposited in the GEO public database (accession #GSE8704).

Western Blot and Immunoprecipitation-Western Blot Analysis

Immunoprecipitations, western blot analysis, and immunoprecipitation-western blot analyses were performed by standard methods and have been described previously (Lu et al., 2005). Antibodies were obtained from commercial sources. These are listed in the next section. Note that 4B2 and 2A9 antibodies (Calbiochem) were mixed and used to immunoprecipitate or immunoblot total Mdm2, and 2A10 antibody was only used to detect nonphosphorylated Mdm2.

Antibodies and Purified Proteins

Anti-p53 (#9292 and #2524) and anti-p53(p15S) (#9286) were purchased from Cell Signaling Technology; anti-actin (#1616), anti-ATM (#23921), anti-ubiquitin (#8017), HRP-anti-goat IgG (#2020), HRP-anti-rabbit IgG (#2302), and HRP-anti-mouse IgG (#2302) were purchased from Santa Cruz; anti-HAUSP (#A300-033A) and anti-HA (A190-108A) were purchased from Bethyl Laboratories; anti-FLAG (#V8012) and anti-V5 (#P2963) were purchased from Sigma-Aldrich; anti-Wip1 (#2380-MC-100) was purchased from Trevigen; anti-Mdm2 (2A10, 4B2, and 2A9), purified PP1 (#539493), and PP2Cα (#539569) were obtained from Calbiochem. PP2A (#14-165) was obtained from Upstate. For the Mdm2 protein blots on *Wip1*$^{-/-}$ MEFs in Figure 1C, the Mdm2 antibodies used were from Santa Cruz (Mdm2 C-18 and Mdm2 K-20 mixed together 1:1). For the mouse spleen western blots in Figure 7B, Mdm2 antibodies C-18, K-20, and H221 from Santa Cruz were mixed in 1:1:1 ratios. The p53 antibody in this experiment was p53 AB1 and AB3 from Calbiochem mixed in a 1:1 ratio. The anti-p53(pS18) antibody used was catalog number 9284 from Cell Signaling Technology.

Protein Stability Measurement

P53$^{-/-}$*Mdm2*$^{-/-}$ MEFs were transfected with expression vector DNA containing wild-type Mdm2, Mdm2 (S395A), or Mdm2 (S395D), with or without Wip1 expression vector DNA. Twenty-four hours after transfection, cells were treated with 5 Gy IR. Cells were pulse labeled in a medium containing ^{35}S-L-methionine and ^{35}S-L-cysteine for 1 hr and then changed to the regular culture medium. Cells were harvested at the indicated time points after labeling, and cell lysates were immunoprecipitated with Mdm2 antibodies. Mdm2 immunoprecipitates were run in the SDS-PAGE. The levels of Mdm2 at each time point were quantitated by phosphorimager for Mdm2 bands on SDS-PAGE gels.

In Vitro Phosphatase Assays

The in vitro phosphatase assays have been described previously (Lu et al., 2004). Mdm2 phosphopeptide (Ac-ESEDYpSQPSTS-amide) was custom synthesized by New England Peptide. Intact Mdm2 proteins were immunopurified with anti-Mdm2 antibodies.

Ubiquitination Assays

Cells were treated with proteasome inhibitors MG101 (25 μM) and MG132 (25 μM). Six hours after treatment, cells were harvested and lysed in the lysis buffer (20 mM HEPES [pH 7.4], 240 mM NaCl, 0.1 mM EDTA, 0.5% Triton X-100 or 0.1% SDS, 1 mM PMSF, 1 mM DTT, and Complete Mini protease inhibitor tablet from Roche). Ubiquitinated p53 was immunoprecipitated with anti-p53 (#126, Santa Cruz) and then was western blot analyzed with anti-ubiquitin antibody (#P4D1, Santa Cruz). Ubiquitinated Mdm2 was immunoprecipitated with anti-HA antibody (against HA-ubiquitin) and then western blot analyzed with anti-Mdm2 (4B2 and 2A6 from Calbiochem) antibodies.

ACKNOWLEDGMENTS

We thank L. Moore for help with ubiquitination studies and C. Gatza, M. Weiss, and L. Moore in our laboratory and L. Liles and L. White in the BCM Microarray Core for their technical assistance. We thank K. Vousden and Y. Minami for generously providing us with p53 phosphorylation mutant constructs and a human Wip1 phosphatase-dead mutant construct. We thank M. Kastan for provision of ATM constructs and B. Vogelstein for supplying an Mdm2 construct. We thank G. Lozano for a p21 promoter luciferase construct. We are also grateful to R. Sutton for provision of retroviral vector constructs. We thank C. Zhu for provision of the ATM null mice. This research was supported by grants to L.A.D. and M.O. from the National Institutes of Health, a grant to X.L. from the A-T Children's Project, and a predoctoral fellowship to T.-A.N. from the Department of Defense Breast Cancer Research Program.

Received: December 11, 2006
Revised: July 23, 2007
Accepted: August 29, 2007
Published: October 15, 2007

REFERENCES

Appella, E., and Anderson, C.W. (2001). Post-translational modifications and activation of p53 by genotoxic stresses. Eur. J. Biochem. *268*, 2764–2772.

Belova, G.I., Demidov, O.N., Fornace, A.J., Jr., and Bulavin, D.V. (2005). Chemical inhibition of Wip1 phosphatase contributes to suppression of tumorigenesis. Cancer Biol. Ther. *4*, 1154–1158.

Bode, A.M., and Dong, Z. (2004). Post-translational modification of p53 in tumorigenesis. Nat. Rev. Cancer *4*, 793–805.

Bond, G.L., Hu, W., and Levine, A.J. (2005). MDM2 is a central node in the p53 pathway: 12 years and counting. Curr. Cancer Drug Targets *5*, 3–8.

Bulavin, D.V., Demidov, O.N., Saito, S., Kauraniemi, P., Phillips, C., Amundson, S.A., Ambrosino, C., Sauter, G., Nebreda, A.R., Anderson, C.W., et al. (2002). Amplification of PPM1D in human tumors abrogates p53 tumor-suppressor activity. Nat. Genet. *31*, 210–215.

Bulavin, D.V., Phillips, C., Nannenga, B., Timofeev, O., Donehower, L.A., Anderson, C.W., Appella, E., and Fornace, A.J., Jr. (2004). Inactivation of the Wip1 phosphatase inhibits mammary tumorigenesis through p38 MAPK-mediated activation of the p16(Ink4a)-p19(Arf) pathway. Nat. Genet. *36*, 343–350.

Canman, C.E., Lim, D.S., Cimprich, K.A., Taya, Y., Tamai, K., Sakaguchi, K., Appella, E., Kastan, M.B., and Siliciano, J.D. (1998). Activation of the ATM kinase by ionizing radiation and phosphorylation of p53. Science *281*, 1677–1679.

Chehab, N.H., Malikzay, A., Appel, M., and Halazonetis, T.D. (2000). Chk2/hCds1 functions as a DNA damage checkpoint in G(1) by stabilizing p53. Genes Dev. *14*, 278–288.

Choi, J., Appella, E., and Donehower, L.A. (2000). The structure and expression of the murine wildtype p53-induced phosphatase 1 (Wip1) gene. Genomics *64*, 298–306.

Choi, J., Nannenga, B., Demidov, O.N., Bulavin, D.V., Cooney, A., Brayton, C., Zhang, Y., Mbawuike, I.N., Bradley, A., Appella, E., and Donehower, L.A. (2002). Mice deficient for the wild-type p53-induced phosphatase gene (Wip1) exhibit defects in reproductive organs, immune function, and cell cycle control. Mol. Cell. Biol. *22*, 1094–1105.

Crook, T., Marston, N.J., Sara, E.A., and Vousden, K.H. (1994). Transcriptional activation by p53 correlates with suppression of growth but not transformation. Cell *79*, 817–827.

Demidov, O.N., Kek, C., Shreeram, S., Timofeev, O., Fornace, A.J., Appella, E., and Bulavin, D.V. (2007). The role of the MKK6/p38 MAPK pathway in Wip1-dependent regulation of ErbB2-driven mammary gland tumorigenesis. Oncogene *26*, 2502–2506. Published online October 2, 2006. 10.1038/sj.onc.1210032.

Fiscella, M., Zhang, H., Fan, S., Sakaguchi, K., Shen, S., Mercer, W.E., Vande Woude, G.F., O'Connor, P.M., and Appella, E. (1997). Wip1, a novel human protein phosphatase that is induced in response to ionizing radiation in a p53-dependent manner. Proc. Natl. Acad. Sci. USA *94*, 6048–6053.

Fujimoto, H., Onishi, N., Kato, N., Takekawa, M., Xu, X.Z., Kosugi, A., Kondo, T., Imamura, M., Oishi, I., Yoda, A., and Minami, Y. (2006). Regulation of the antioncogenic Chk2 kinase by the oncogenic Wip1 phosphatase. Cell Death Differ. *13*, 1170–1180. Published online November 25, 2005. 10.1038/sj.cdd.4401801.

Harris, S.L., and Levine, A.J. (2005). The p53 pathway: Positive and negative feedback loops. Oncogene *24*, 2899–2908.

Hirao, A., Kong, Y.Y., Matsuoka, S., Wakeham, A., Ruland, J., Yoshida, H., Liu, D., Elledge, S.J., and Mak, T.W. (2000). DNA damage-induced activation of p53 by the checkpoint kinase Chk2. Science *287*, 1824–1827.

Hirasawa, A., Saito-Ohara, F., Inoue, J., Aoki, D., Susumu, N., Yokoyama, T., Nozawa, S., Inazawa, J., and Imoto, I. (2003). Association of 17q21-q24 gain in ovarian clear cell adenocarcinomas with poor prognosis and identification of PPM1D and APPBP2 as likely amplification targets. Clin. Cancer Res. *9*, 1995–2004.

Jones, S.N., Sands, A.T., Hancock, A.R., Vogel, H., Donehower, L.A., Linke, S.P., Wahl, G.M., and Bradley, A. (1996). The tumorigenic potential and cell growth characteristics of p53-deficient cells are equivalent in the presence or absence of Mdm2. Proc. Natl. Acad. Sci. USA *93*, 14106–14111.

Lane, D.P. (2005). Exploiting the p53 pathway for the diagnosis and therapy of human cancer. Cold Spring Harb. Symp. Quant. Biol. *70*, 489–497.

Lavin, M.F., and Gueven, N. (2006). The complexity of p53 stabilization and activation. Cell Death Differ. *13*, 941–950.

Li, J., Yang, Y., Peng, Y., Austin, R.J., van Eyndhoven, W.G., Nguyen, K.C., Gabriele, T., McCurrach, M.E., Marks, J.R., Hoey, T., et al. (2002). Oncogenic properties of PPM1D located within a breast cancer amplification epicenter at 17q23. Nat. Genet. *31*, 133–134.

Li, M., Brooks, C.L., Kon, N., and Gu, W. (2004). A dynamic role of HAUSP in the p53-Mdm2 pathway. Mol. Cell *13*, 879–886.

Lu, X., Bocangel, D., Nannenga, B., Yamaguchi, H., Appella, E., and Donehower, L.A. (2004). The p53-induced oncogenic phosphatase PPM1D interacts with uracil DNA glycosylase and suppresses base excision repair. Mol. Cell *15*, 621–634.

Lu, X., Nguyen, T.A., and Donehower, L.A. (2005). Reversal of the ATM/ATR-mediated DNA damage response by the oncogenic phosphatase PPM1D. Cell Cycle *4*, 1060–1064.

Martin, A.C., Facchiano, A.M., Cuff, A.L., Hernandez-Boussard, T., Olivier, M., Hainaut, P., and Thornton, J.M. (2002). Integrating mutation data and structural analysis of the TP53 tumor-suppressor protein. Hum. Mutat. *19*, 149–164.

Maya, R., Balass, M., Kim, S.T., Shkedy, D., Leal, J.F., Shifman, O., Moas, M., Buschmann, T., Ronai, Z., Shiloh, Y., et al. (2001). ATM-dependent phosphorylation of Mdm2 on serine 395: Role in p53 activation by DNA damage. Genes Dev. *15*, 1067–1077.

Meek, D.W., and Knippschild, U. (2003). Posttranslational modification of MDM2. Mol. Cancer Res. *1*, 1017–1026.

Mendrzyk, F., Radlwimmer, B., Joos, S., Kokocinski, F., Benner, A., Stange, D.E., Neben, K., Fiegler, H., Carter, N.P., Reifenberger, G., et al. (2005). Genomic and protein expression profiling identifies CDK6 as novel independent prognostic marker in medulloblastoma. J. Clin. Oncol. *23*, 8853–8862.

Meulmeester, E., Maurice, M.M., Boutell, C., Teunisse, A.F., Ovaa, H., Abraham, T.E., Dirks, R.W., and Jochemsen, A.G. (2005). Loss of HAUSP-mediated deubiquitination contributes to DNA damage-induced destabilization of Hdmx and Hdm2. Mol. Cell *18*, 565–576.

Michael, D., and Oren, M. (2003). The p53-Mdm2 module and the ubiquitin system. Semin. Cancer Biol. *13*, 49–58.

Moll, U.M., and Petrenko, O. (2003). The MDM2-p53 interaction. Mol. Cancer Res. *1*, 1001–1008.

Momand, J., Jung, D., Wilczynski, S., and Niland, J. (1998). The MDM2 gene amplification database. Nucleic Acids Res. *26*, 3453–3459.

Mumby, M.C., and Walter, G. (1993). Protein serine/threonine phosphatases: Structure, regulation, and functions in cell growth. Physiol. Rev. *73*, 673–699.

Nannenga, B., Lu, X., Dumble, M., Van Maanen, M., Nguyen, T.A., Sutton, R., Kumar, T.R., and Donehower, L.A. (2006). Augmented cancer resistance and DNA damage response phenotypes in PPM1D null mice. Mol. Carcinog. *45*, 594–604.

Ofek, P., Ben-Meir, D., Kariv-Inbal, Z., Oren, M., and Lavi, S. (2003). Cell cycle regulation and p53 activation by protein phosphatase 2C alpha. J. Biol. Chem. *278*, 14299–14305.

Okamoto, K., Li, H., Jensen, M.R., Zhang, T., Taya, Y., Thorgeirsson, S.S., and Prives, C. (2002). Cyclin G recruits PP2A to dephosphorylate Mdm2. Mol. Cell *9*, 761–771.

Oliva-Trastoy, M., Berthonaud, V., Chevalier, A., Ducrot, C., Marsolier-Kergoat, M.C., Mann, C., and Leteurtre, F. (2006). The Wip1 phosphatase (PPM1D) antagonizes activation of the Chk2 tumour suppressor kinase. Oncogene *26*, 1449–1458.

Saito-Ohara, F., Imoto, I., Inoue, J., Hosoi, H., Nakagawara, A., Sugimoto, T., and Inazawa, J. (2003). PPM1D is a potential target for 17q gain in neuroblastoma. Cancer Res. *63*, 1876–1883.

Sanchez-Prieto, R., Rojas, J.M., Taya, Y., and Gutkind, J.S. (2000). A role for the p38 mitogen-acitvated protein kinase pathway in the transcriptional activation of p53 on genotoxic stress by chemotherapeutic agents. Cancer Res. *60*, 2464–2472.

Sekiguchi, J., Ferguson, D.O., Chen, H.T., Yang, E.M., Earle, J., Frank, K., Whitlow, S., Gu, Y., Xu, Y., Nussenzweig, A., and Alt, F.W. (2001). Genetic interactions between ATM and the nonhomologous end-joining factors in genomic stability and development. Proc. Natl. Acad. Sci. USA *98*, 3243–3248.

Shiloh, Y. (2003). ATM and related protein kinases: Safeguarding genome integrity. Nat. Rev. Cancer *3*, 155–168.

Shreeram, S., Demidov, O.N., Hee, W.K., Yamaguchi, H., Onishi, N., Kek, C., Timofeev, O.N., Dudgeon, C., Fornace, A.J., Anderson, C.W., et al. (2006). Wip1 phosphatase modulates ATM-dependent signaling pathways. Mol. Cell *23*, 757–764.

Sluss, H.K., Armata, H., Gallant, J., and Jones, S.N. (2004). Phosphorylation of serine 18 regulates distinct p53 functions in mice. Mol. Cell. Biol. *24*, 976–984.

Stommel, J.M., and Wahl, G.M. (2005). A new twist in the feedback loop: Stress-activated MDM2 destabilization is required for p53 activation. Cell Cycle *4*, 411–417.

Takekawa, M., Adachi, M., Nakahata, A., Nakayama, I., Itoh, F., Tsukuda, H., Taya, Y., and Imai, K. (2000). p53-inducible wip1 phosphatase mediates a negative feedback regulation of p38 MAPK-p53 signaling in response to UV radiation. EMBO J. *19*, 6517–6526.

Tibbetts, R.S., Brumbaugh, K.M., Williams, J.M., Sarkaria, J.N., Cliby, W.A., Shieh, S.Y., Taya, Y., Prives, C., and Abraham, R.T. (1999). A role for ATR in the DNA damage-induced phosphorylation of p53. Genes Dev. *13*, 152–157.

Toledo, F., and Wahl, G.M. (2006). Regulating the p53 pathway: In vitro hypotheses, in vivo veritas. Nat. Rev. Cancer *6*, 909–923.

Vogelstein, B., Lane, D., and Levine, A.J. (2000). Surfing the p53 network. Nature *408*, 307–310.

Yamaguchi, H., Durell, S.R., Feng, H., Bai, Y., Anderson, C.W., and Appella, E. (2006). Development of a substrate-based cyclic phosphopeptide inhibitor of protein phosphatase 2Cdelta, Wip1. Biochemistry *45*, 13193–13202.

Yoda, A., Xu, X.Z., Onishi, N., Toyoshima, K., Fujimoto, H., Kato, N., Oishi, I., Kondo, T., and Minami, Y. (2006). Intrinsic kinase activity and SQ/TQ domain of Chk2 kinase as well as N-terminal domain of Wip1 phosphatase are required for regulation of Chk2 by Wip1. J. Biol. Chem. *281*, 24847–24862.

Yu, Q., La Rose, J., Zhang, H., Takemura, H., Kohn, K.W., and Pommier, Y. (2002). UCN-01 inhibits p53 up-regulation and abrogates gamma-radiation-induced G(2)-M checkpoint independently of p53 by targeting both of the checkpoint kinases, Chk2 and Chk1. Cancer Res. *62*, 5743–5748.

Accession Numbers

The raw data for the microarray analyses have been deposited in the GEO public database (accession #GSE8704).